Title	Determination of Temperature and Fuel Utilization Distributions in SOFC Stacks with EIS
Author(s)	Tallgren, Johan; Boigues Muñoz, Carlos; Mikkola, Jyrki; Himanen, Olli; Kiviaho, Jari
Citation	ECS Transactions. The Electrochemical Society . Vol. 78 (2017) No: 1, 2141-2150
Date	2017
URL	http://dx.doi.org/10.1149/07801.2141ecst
Rights	This post-print version of the article may be downloaded for personal use only.

Determination of Temperature and Fuel Utilization Distributions in SOFC Stacks with EIS

J. Tallgren[a], C. Boigues Muñoz[b], J. Mikkola[a], O. Himanen[a], and J. Kiviaho[a]

[a] VTT Technical Research Centre of Finland Ltd, P.O. Box 1000, Biologinkuja 5, Espoo, FI-02044, Finland

[b] ENEA, Via Anguillarese 301, 00123 Rome, Italy

Efficient operation of solid oxide fuel cell (SOFC) stacks requires uniform temperature and fuel utilization distributions in the stack. Especially high fuel utilizations necessitate uniform fuel flow distributions to avoid performance decrease or anode reoxidation. A uniform temperature distribution helps to prolong the life-time of the stack. This work presents a method to determine the fuel utilization and temperature distribution in SOFC stacks with electrochemical impedance spectroscopy (EIS). The equations for relating the measured impedance and fuel utilization and temperature are derived from physical equations describing the SOFC stack. The method is demonstrated with an ElringKlinger AG 10-cell stack fuelled with 50%/50% H_2/N_2 at nominal operation conditions. The difference in temperature and fuel utilization between cells was determined. The calculated distributions are in line with cell voltage measurements. The method can be used to improve SOFC stack design and performance.

Introduction

Solid oxide fuel cells (SOFC) are seen as a promising technology in reducing emissions in energy production but its full scale market penetration is delayed by issues related to durability and cost (1–3). In addition to overcome the current obstacles, it is of importance to optimize the operation and design of the stack to realize the possibilities of high efficiency and required lifetime. High stack efficiency calls for high fuel utilizations, which in turn necessitate uniform fuel flow distributions within the stack to avoid performance decrease due to fuel starvation. In worst case, anode reoxidation can take place in the cell with the highest local fuel utilization (FU). Fuel flow distributions are affected by the stack design, in particular pressure drop over the gas channels and adjacent manifold channels. Stack design is aided by e.g. CFD modelling but non-optimal fuel flow distributions might be hard to distinguish from other factors affecting the performance in common stack characterization measurements. Uniform temperature distributions are of interest to prolong the stack lifetime. High temperature gradients contribute to increased thermal stress, uneven electrochemical activity, and possibly stack damages due to mismatched thermal expansion coefficients of components. Thermal gradients can be induced to the stack due to causes related both to stack design and operation. Also internal reforming increases thermal gradients in the stack.

Stack temperature distributions have been determined by either direct measurement with specially built stacks incorporating thermocouples (4–7) or by different modelling approaches, such as numerical, CFD or data-based modelling (8–11). However, inserting

thermocouples in the stack or manufacturing thicker interconnect plates with inserts for thermocouples may change the stack properties and yield different results than with the original stack. Electrochemical impedance spectroscopy (EIS) has been used to determine the temperature of unit cells at nominal operation conditions, for example by Klotz et al (12,13), who have used single-frequency EIS with frequencies above 100 kHz. However, such high frequencies are affected by noise, which becomes cumbersome particularly when studying larger stacks instead of single cells.

This work presents a method to determine the fuel utilization and temperature distribution in SOFC stacks with electrochemical impedance spectroscopy (EIS). Previously, Dekker et al (14) presented the basic idea of determining the anode gas flow distribution and Mosbæk et al (15) have shown the correlation of low frequency responses to changes in gas supply over individual cells. This work refines the methodology presented by Dekker et al and extends it to cover also temperature distributions, which have not previously been reported. EIS is a powerful and non-destructive technique that enables an in-depth analysis of the stack in-operando at nominal operation conditions. The measurement method is based on the relation between EIS low frequency response and fuel utilization of a cell and between the ionic and electronic conductivity and the temperature (16–20). The EIS low frequency response is also called gas conversion impedance. The equations for relating the measured impedance and fuel utilization and temperature are derived from common equations describing the SOFC stack, namely Fick's diffusion equation and the Arrhenius type of equation for conductivity. Knowledge about the distributions can aid in both stack design and in monitoring the "state-of-health" of stacks. This article presents the method and demonstrates it on an ElringKlinger AG 10-cell stack.

Methodology

The inherent properties of electrochemical systems can be studied by electrochemical impedance spectroscopy (EIS) and the different electrochemical processes can be distinguished. The measurement methodology reported here is based on fuel utilization being related to the gas conversion impedance. As the electric current through all cells is equal, also a fuel gas flow distribution can be calculated from the gas conversion impedance. Furthermore, the temperature is related to the ohmic cell resistance, which corresponds to the EIS high frequency response. To determine a numerical value for the gas conversion impedance and the ohmic resistance, the measured EIS spectra was fitted to a simple equivalent circuit for describing the SOFC. The circuit consists of one serial resistance and two parallel constant phase element–resistor circuits, as illustrated in Figure 1. In the figure, R_s represents the ohmic resistance, the first parallel circuit R_1-CPE_1 represents gas-solid interactions at the electrodes and the second parallel circuit R_2-CPE_2 represents gas conversion. Here the real part of gas conversion impedance, R_2, will be used in the calculations.

As described by Dekker et al, the determination of the distributions is a stepwise process:

1. Measure EIS spectra for different temperatures and fuel utilizations of an average cell, e.g. the middle cell, and fitting these spectra to the equivalent circuit.
2. Determine a relation between temperature and the measured values of R_s as well as fuel utilization and R_2 by fit corresponding equations with the data.

3. Measure EIS of all cells at nominal operation condition and use the relation determined in step 2 to calculate temperature and fuel utilization of each cell.

In case the stack FU does not match with the average cell FU, the input in the first step should be normalized and the distributions recalculated. The next two sections detail how the relations for fuel utilization distribution and temperature distribution are determined.

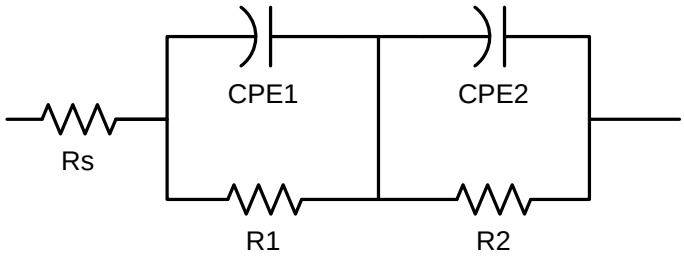

Figure 1. Equivalent circuit describing solid oxide fuel cells, consisting of a serial resistance and two parallel resistor-constant phase element circuits.

Fuel utilization distribution

The equation relating fuel flow distribution to gas conversion impedance is determined from Fick's diffusion law, describing the gas diffusion at the fuel electrode. Fickian diffusion in a ternary gaseous mixture (take generic components *k*, *l* and *m*) is expressed as follows in the one-dimensional domain and in porous media:

$$\frac{PD_{k,T}^{eff}}{RT}\frac{d^2x_k}{dz^2} = 0 \quad [1]$$

where *P* is the total pressure, *R* is the ideal gas constant, *T* the operating temperature, x_k is the molar fraction of component *k*, *z* is the position along the thickness of the anode and $D_{k,T}^{eff}$ is the effective binary diffusivity of component *k*, which can be written in the following terms:

$$D_{k,T}^{eff} = \left(\frac{1}{D_{Kn,k}^{eff}} + \frac{1}{D_{k,m}^{eff}} + \frac{1}{D_{k,l}^{eff}} - (1 - x_m)\frac{1}{D_{k,m}^{eff}}\right)^{-1} \quad [2]$$

where $D_{k,l}^{eff}$ and $D_{k,m}^{eff}$ are the effective molecular diffusions and $D_{Kn,k}^{eff}$ is the effective Knudsen diffusion of component *k*.

For simplicity issues, it can be assumed that the electrochemical reaction in the anode of the solid oxide fuel cell occurs in the interface between the anode and the electrolyte. Taking this into consideration, the Neumann boundary condition is expressed by means of Eq. 3, and the Dirichlet boundary condition is given by Eq. 4.

$$\left.\frac{dx_{H2}}{dz}\right|_{z=L} = -\frac{IRT}{2FPD_{H2,T}^{eff}} \quad [3]$$

where I is the current generated by the SOFC and F is Faraday's constant.

$$x_{H2}|_{z=0} = x_{H2}^{bulk} \quad [4]$$

where x_{H2}^{bulk} is the molar fraction of hydrogen in the inlet of the stack. The Neumann boundary condition describes that the gradient of hydrogen fraction, i.e. the hydrogen flux, at the boundary between anode and electrolyte is determined by the electric current. The Dirichlet boundary condition describes that hydrogen concentration at the anode boundary is equal to the hydrogen concentration in the gas channels.

The ordinary differential equation (ODE) can thus be solved, taking the following form:

$$x_{H2} = x_{H2}^{bulk} - \frac{IRT}{2FPD_{H2,T}^{eff}} z \quad [5]$$

The concentration overpotential of the negative electrode is expressed by Eq. 6.

$$\eta_{conc,anode} = \frac{RT}{2F} \ln\left(\frac{x_{H2}^{bulk} \cdot x_{H2O}}{x_{H2} \cdot x_{H2O}^{bulk}}\right) \quad [6]$$

It is immediate to define $\eta_{conc,anode}$ as a function of the current being generated by substituting Eq. 5 into Eq. 6 and taking into consideration that $x_{H2} + x_{H2O} + x_{N2} = 1 \quad \forall z$. Hence, the resistance associated to the concentration overpotential at the anode-electrolyte interface is expressed in the following terms:

$$r_{conc,anode} = \frac{d\eta_{conc,anode}}{dI} = \frac{RT}{2F} \frac{\left(1 - x_{N2}^{bulk}\right) \frac{RT}{2FPD_{H2,T}^{eff}} L}{\left(x_{H2O}^{bulk} + \frac{IRT}{2FPD_{H2,T}^{eff}} L\right)\left(x_{H2}^{bulk} - \frac{IRT}{2FPD_{H2,T}^{eff}} L\right)} \quad [7]$$

Once $r_{conc,anode}$ has been obtained, it can be reformulated to be expressed in terms of the fuel utilization. Recalling the expression for the fuel utilization, (Eq. 8),

$$U_f = \frac{IRT}{2FPf_{neg,cell}x_{H2}^{bulk}} \quad [8]$$

where $f_{neg,cell}$ is the total volumetric flow rate entering the negative electrode of a cell.

Therefore, $r_{conc,anode}$ in terms of the fuel utilization takes the following form:

$$r_{conc,anode} = \frac{RT}{2F} \frac{\left(1 - x_{N2}^{bulk}\right) \frac{RT}{2FPD_{k,T}^{eff}} L}{\left(x_{H2O}^{bulk} + \frac{f_{neg,cell} x_{H2}^{bulk} FU}{D_{H2,T}^{eff}} L\right)\left(x_{H2}^{bulk} - \frac{f_{neg,cell} x_{H2}^{bulk} FU}{D_{H2,T}^{eff}} L\right)} \quad [9]$$

The fuel utilization can be expressed in term of the concentration resistance. By lumping the coefficients and parameters into generic constants, the following equation arises:

$$r_{conc,anode} = \frac{1}{aFU^2 + bFU + c} \quad [10]$$

Since the gas flow to the cathode is kept constant, only variations in the anode gas flow affect the gas conversion impedance, and $r_{conc,anode}$ can be described with GCI.

Temperature distribution

The relation describing temperature as function of the serial resistance R_s is based on the Arrhenius conductivity equation (Eq. 11)

$$\sigma T = \sigma_0 \exp\left(\frac{E_a}{k_B T}\right) \quad [11]$$

where σ is the conductivity, T is the temperature in Kelvin, σ_0 is a material constant, E_a is the activation energy and k_B is the Boltzmann constant. Simplifying the relation by the following steps

$$\frac{T}{R} = \sigma_0 \exp\left(\frac{E_a}{k_B T}\right)$$

$$R \propto \exp(T)$$

$$T \propto \ln(R) \quad [12]$$

yields a logarithmic relation for the temperature as function of the serial resistance with the generic constants A and B (Eq 13):

$$T = A \ln(R_s) + B \quad [13]$$

Experimental setup

The measurements were performed on an ElringKlinger C-design 10 cell stack. The stack was placed in a furnace (MeyerVastus) and fed with air and a fuel mixture consisting of 50%/50% H_2/N_2 through mass flow controllers (Bronkhorst EL-FLOW). The stack was connected to an electric load (Kikusui PLZ1004). At nominal operation conditions,

furnace temperature was held at 700 ºC, fuel feed was 3.5 l_N/min H_2, 3.5 l_N/min H_2 and air feed was 30 l_N/min. The current was 25.2 A, which corresponds to a current density of 0.3 A/cm^2. EIS was measured with a five-channel impedance monitor (ZiveLabs Z#). Measured frequency range was 10 mHz – 30 kHz, with DC component 25.2 A and AC component 0.8 A. The cells were grouped in cell blocks so that cell 1, cells 2-4, cells 5-6, cells 7-9 and cell 10 formed five blocks. Kramers-Kronig relations were used to validate the data. Data points with relative residuals higher than ±1% were discarded. The data was fitted with ZiveLab's software ZMAN to the equivalent circuit illustrated in Figure 1.

As the fuel utilization at nominal operation conditions was 50%, it was varied from 30% to 70%, with steps of 10 percentage units, for determining the parameters in Eq 10. Similarly, furnace temperature was varied from 650 °C to 750 °C with 25 °C steps to determine the parameters for Eq. 13. The stack temperature was determined as the average of inlet and outlet air temperature.

Results and discussion

An IV curve was recorded in the beginning of the test, presented in Figure 2. The measured EIS spectra were fitted to the equivalent circuit shown in Figure 1. The obtained values for R_s and R_2 from the middle cell block, containing cells 5 and 6, were used for determining the parameters to equations 10 and 13. The middle cells should be representative for the stack with regard to fuel flow and temperature, and as seen in the IV curve in Figure 2, their performance is in the same range as the other cells. From the IV curve it is seen that all cells apart from cell 1 show similar voltages over the current range. Cell 1 shows the lowest performance over the whole current range and cell 10 is the first to show signs of fuel shortage.

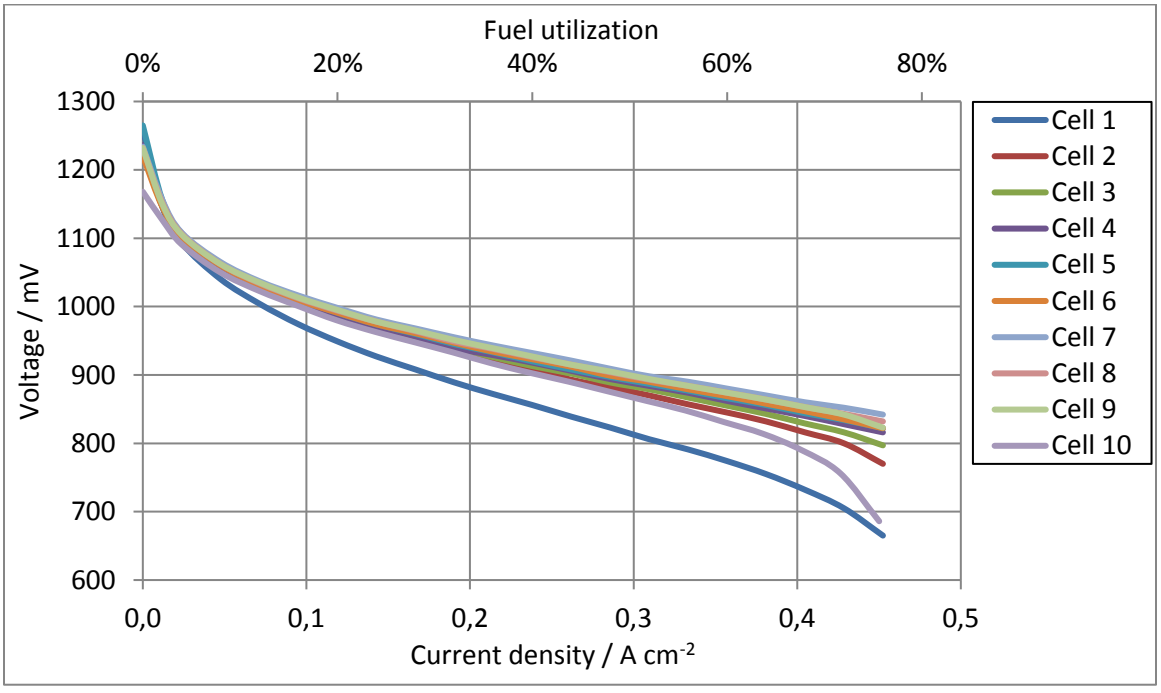

Figure 2. IV curve recorded in the beginning of the test at 700 °C. (For the color graph, the reader is advised to the electronic publication.)

Figure 3 presents the equation fitting to the measured values. Figure 3a illustrates the measured gas conversion impedance at different fuel utilizations and 3b shows the logarithmic dependency of temperature and serial resistance. The obtained equations fit closely to the measured data.

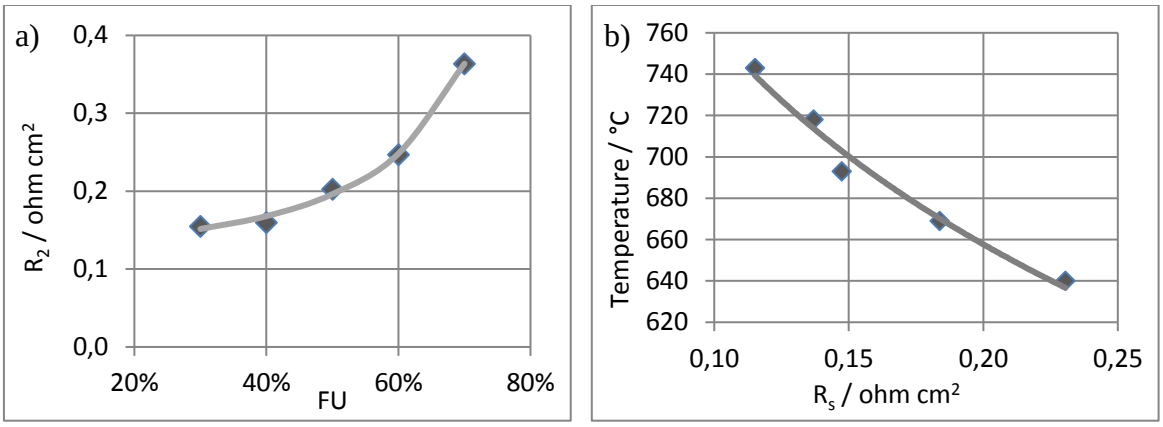

Figure 3. Fitting equations 10 and 13 to the measured impedance data: a) gas conversion impedance at different FU and b) temperature related to serial resistance.

Figure 4 presents the calculated fuel flow over the anode in each cell group. The gas flow is normalized with respect to the number of cells in the group. The highest gas flows are seen in the middle of the stack and the outermost cells receive less fuel. The feed to cells 7-9 is 770 ml/min and 610 ml/min to cell 10. The uncertainty of the calculated fuel flow is estimated to ±6%. Errors may be induced from faults in EIS spectra which are small enough to be approved in the Kramers-Kronig test, errors from fitting the spectra to the equivalent circuit, errors from fitting equations 10 and 13 to the measured R_s and R_2 values and mass flow controller uncertainty. Taking the uncertainty limits into account, the distribution could be smoother. However, the distribution is in correspondence with the IV curve in Figure 2 where it is seen that cell 10 is the first to show signs of fuel shortage.

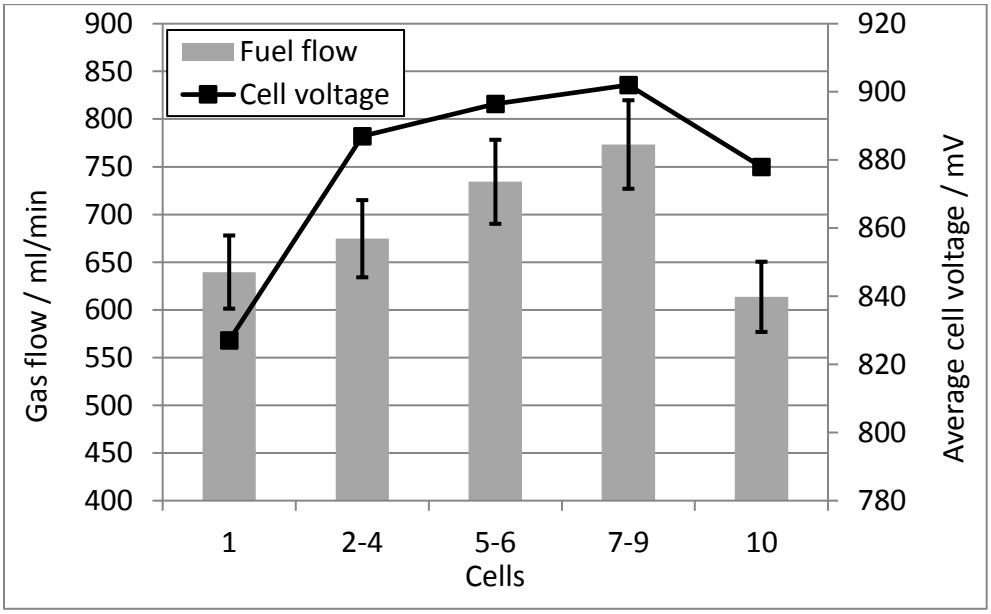

Figure 4. Calculated anode fuel flow distribution over each cell group compared with measured average cell voltage in corresponding cell group.

The average cell voltage of each block is also plotted in the graph. The voltage distribution follows the fuel flow distribution roughly, but there are some discrepancies to be seen, e.g. for cells 1 and 10. This suggests that there is another governing mechanism, for example temperature. It should be noted that the fuel gas distribution shown here holds only for the 10-cell ElringKlinger stack and has been improved after the measurements reported here.

Calculated temperature distribution is illustrated in Figure 5. As above, the results are normalized for individual cells. The graph shows that the temperature is highest in the middle of the stack and decrease towards the ends of the stack. The maximal temperature difference is 60 °C with cell 1 being the coolest. Probable reasons are that the gases enter the stack from below and that the stack stand goes through the furnace bottom and may act as a thermal bridge, as cell 1 is the bottommost cell. The uncertainty of the calculated values is estimated to 3%, stemming from the error sources as described above, except for mass flow controller uncertainty. The total error could be decreased by performing a greater amount of measurement to increase sample size and by optimizing the EIS measurement setup.

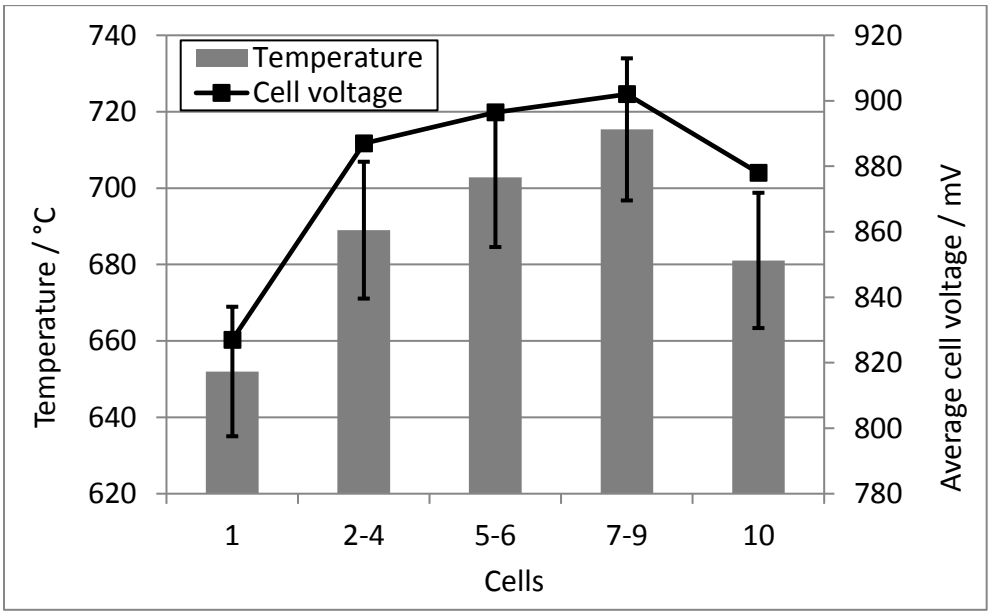

Figure 5. Calculated temperature distribution over each cell group compared with measured average cell voltage in corresponding cell group.

Figure 5 also depicts the average cell voltage for each cell block. Here it is seen that the voltages follow the temperature distribution. Thus, it can be concluded that the temperature affects voltages more than the fuel utilization at moderate fuel utilizations. This is also supported by the IV curve in which cell 1 shows the lowest voltage but only small signs of fuel shortage at high currents. Figure 4 also shows that fuel flow to cell 1 is higher to cell 10, thus explaining the smaller voltage drop at high FU. Since the temperatures in the first step for deriving parameters to Eq. 13 are determined as the average of inlet and outlet air temperature, the real cell temperature could be higher. So forth, the most important outcome from Figure 5 is the distribution and not the values themselves. To improve the situation, the temperature could be determined more closely, e.g. by method presented by Klotz et al (12). However, this requires high frequencies to be used,

which is cumbersome in stack test stations due to induced inductive errors that are easier to deal with in single cell test station due to size.

Summary

A method for determining temperature and fuel utilization distributions in SOFC stacks was presented. The method builds on previous research and is extended to cover the temperature distribution. Equations for relating the gas conversion impedance to fuel utilization and the serial resistance to temperature were determined from Fick's diffusion equation and the conductivity equation of Arrhenius type, respectively. The method was demonstrated on an ElringKlinger 10-cell stack. The determined distributions showed that the outermost cells receive less fuel than the average cell and are also the coldest. The distributions correspond to measured IV curves and suggest that the temperature affects cell performance more than the fuel utilization does at nominal operation conditions with conservative fuel utilization. The work could be further improved by optimizing the EIS measurement setup for stack tests and by determining the reference cell temperature more precisely. The method developed in this work can be used to improve and evaluate stack design and so forth increase the performance of SOFC stacks.

Acknowledgments

The NELLHI (grant agreement no. 621227) and INNO-SOFC (grant agreement no. 671403) projects, which have received funding from the European Union's Fuel Cells and Hydrogen Joint Technology Initiative, are acknowledged. Additionally, the STEP project, funded by the Finnish Funding Agency for Innovation TEKES and Projektträger Jülich (Germany), is acknowledged.

References

1. A.B. Stambouli and E. Traversa, *Renew. Sustain. Energy Rev.*, **6**, 433 (2002).
2. S.C. Singhal, *Wiley Interdiscip. Rev. Energy Environ.*, **3,** 179 (2014).
3. T.A. Adams II et al, *Ind. Eng. Chem. Res.*, **52,** 3089 (2013).
4. W.B. Guan et al, *Fuel Cells*, **12,** 24 (2012).
5. O. Razbani et al, *Appl. Energy*, **105,** 155 (2013).
6. M.P. Ranaweera and J.-S. Kim, *ECS Trans.*, **68**(1), 2637 (2015).
7. S. Celik et al, *Int. J. Hydrogen Energy*, **38,** 10534 (2013).
8. P. Vijay et al, *J. Process Control*, **23,** 429 (2013).
9. A. Pohjoranta et al, *J. Power Sources*, **277,** 464 (2015).
10. B. Huang et al, *J. Process Control*, **21,** 1426 (2011).
11. K. Wang et al, *Int. J. Hydrogen Energy*, **36,** 7212 (2011).
12. D. Klotz et al, *Proc. 8th Eur. Fuel Cell Forum*, B0909 (2008).
13. D. Klotz et al, *ECS Trans.* **45**(1), 523 (2012).
14. N.J. Dekker et al, ECS Trans. **25**(2), 1871 (2009).
15. R.R. Mosbæk et al, *Proc. 11th Eur. SOFC SOE Forum*, A0902 (2014).
16. S.H. Jensen et al, *J. Electrochem. Soc.*, **154,** B1325 (2007).
17. A. Momma et al, *Solid State Ionics.*, **174,** 87 (2004).

18. R. Barfod et al, *J. Electrochem. Soc.*, **154**, B371 (2007).
19. Q.-A. Huang et al, *Electrochim. Acta,* **52,** 8144 (2007).
20. S. Primdahl and M. Mogensen, *J. Electrochem. Soc.*, **146,** 2827 (1999).